



Synthesis of artemisinin-piperazine-furan ether hybrids and evaluation of *in vitro* cytotoxic activity



Meng-Xue Wei^{*}, Jia-Ying Yu, Xin-Xin Liu, Xue-Qiang Li, Meng-Wei Zhang, Pei-Wen Yang, Jin-Hui Yang

State Key Laboratory of High-efficiency Utilization of Coal and Green Chemical Engineering, Ningxia Engineering Research Center for Natural Medicine, National Demonstration Center for Experimental Chemistry Education, College of Chemistry and Chemical Engineering, Ningxia University, 489 Helanshan West Road, Yinchuan, 750021, China

ARTICLE INFO

Article history:

Received 8 December 2020

Received in revised form

25 January 2021

Accepted 7 February 2021

Available online 16 February 2021

Keywords:

Furan ether

Artemisinin

X-ray crystallography

Cytotoxic activity

Cancer cells

ABSTRACT

For the first time, eight novel artemisinin-piperazine-furane ether hybrids (**5a–h**) were efficiently synthesized and investigated for their *in vitro* cytotoxic activity against some human cancer and benign cells. The absolute configuration of hybrid **5c** was determined by X-ray crystallographic analysis. Hybrids **5a–h** exhibited more pronounced growth-inhibiting action on hepatocarcinoma cell lines than their parent dihydroartemisinin (DHA) and the reference cytosine arabinoside (ARA). The hybrid **5a** showed the best cytotoxic activity against human hepatocarcinoma cells SMMC-7721 ($IC_{50} = 0.26 \pm 0.03 \mu\text{M}$) after 24 h. Furthermore, hybrid **5a** also showed good cytotoxic activity against human breast cancer cells MCF-7 and low cytotoxicity against human breast benign cells MCF-10A *in vitro*. We found the cytotoxicity of hybrid **5a** did not change when tumour cells absorb iron sulfate (FeSO_4); thus, we conclude the anti-tumour mechanism induced by iron ions (Fe^{2+}) is unclear.

© 2021 Elsevier Masson SAS. All rights reserved.

1. Introduction

Furanone moiety (**1a**, Fig. 1) attracted a lot of attention because of its significant biological activities [1–7] and occurrence in many natural products [8–10]. Natural borneol and menthol are Chinese herbal medicines with anti-inflammatory effects. In previous work, our group found that a single epimer of the chiral furan ethers provides good cytotoxic activity [11,12]. Artemisinin (ARS, **1b**) extracted from *Artemisia annua* is used in Chinese medicine to treat chills and fever [13,14]. Since 1993, a large volume of studies have highlighted the potential of ARS as a novel therapeutic agent for cancer [15–18]. Dihydroartemisinin (DHA, **1c**) exhibited high anticancer activity in Lewis lung carcinoma (LLC) cell line *in vitro* [19]. Artesunate (ART, **1d**) has been reported to kill cancer cells by inducing oxidative stress and DNA damage; it can also down-regulate human recombinant protein in ovarian cancer cells [20]. Over the past decade, hybridization of natural products has proven to be a very effective strategy for medicinal chemistry and drug design. This process not only saves time and cost, but also improves

the pharmacological properties of the parent compound by increasing biological efficacy, reducing adverse side effects, modifying the selectivity spectrum (low toxicity), providing better bioavailability, and introducing new biological properties not found in the parent compound. The combination of artemisinin-type drugs with anticancer drugs can enhance the activity of the anticancer drugs *in vitro* or *in vivo* [21–24].

Given the therapeutic properties of furan derivatives and the lack of artemisinin-piperazine-furan ether hybrids reported in the literature, we designed and synthesized a new series of hybrid furan ether derivatives possessing an artemisinin-piperazine moiety (**5a–h**, Scheme 3) to evaluate their *in vitro* cytotoxicity and compare with VCR and ARA. Then we also research the effects of Fe^{2+} on cytotoxic activity [25–29].

2. Results and discussion

2.1. Synthesis

Compound **2** was synthesized through a substitution reaction [22], using dry dimethyl sulfoxide (DMSO) as a catalyst (Scheme 1). First, DHA and oxalyl chloride formed artemisinin chloroformyl formic ester. Then, the amidogen of piperazine replaced the

^{*} Corresponding author.

E-mail address: weimengxue@nxu.edu.cn (M.-X. Wei).

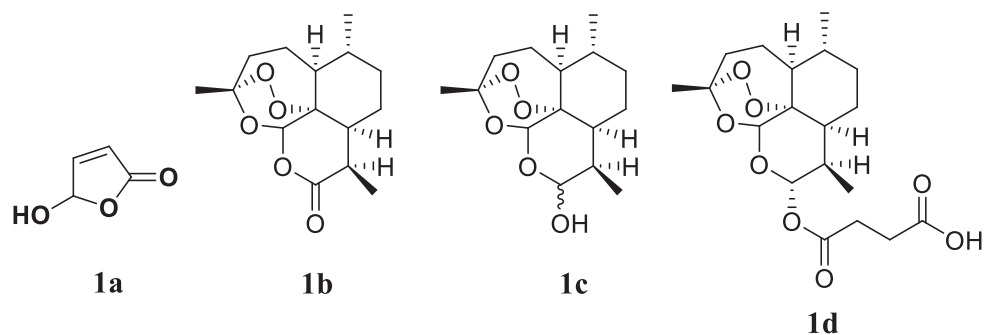
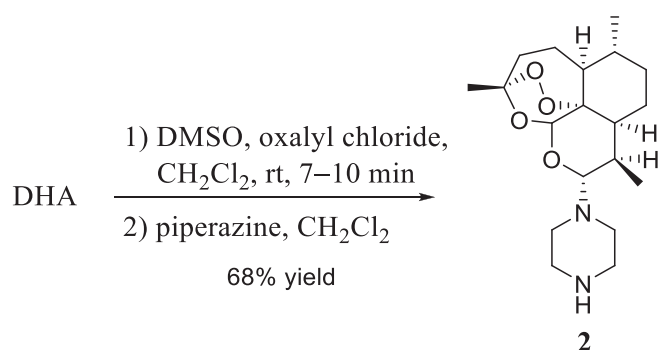


Fig. 1. Structures of furanone (**1a**), artemisinin (ARS, **1b**), dihydroartemisinin (DHA, **1c**), and artesunate (ART, **1d**).



Scheme 1. Synthesis of Compound **2**.

chloroformyl formic ester to produce the artemisinin-piperazine **2** in 68% yield.

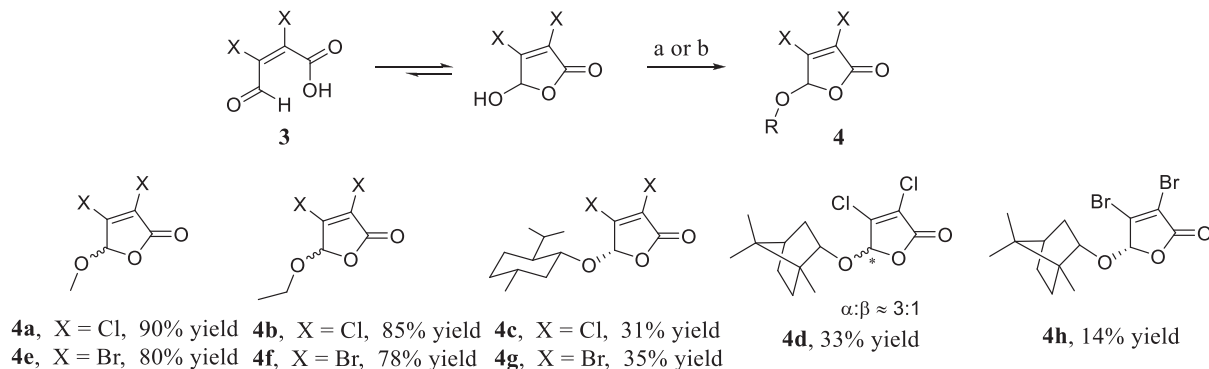
The halogenated furan ethers **4a–h** were synthesized using alcohol and mucochloric acid or mucobromic acid **3** as raw materials and concentrated sulphuric acid as a catalyst (Scheme 2). The reaction requires a water separator to separate the water to move the balance to the right. Because methanol (MeOH) and ethanol (EtOH) are denser than cyclohexane, we chose 1,2-dichloroethane as solvent and added methanol and ethanol at regular intervals to shift the balance to the right. Menthol and borneol would be carbonized when heated under reflux, so the reaction mixture required stirring at room temperature (rt) before heating slowly; however, there was still some carbonization. Intermediate furan ethers were all solid except for **4a** and **4b**. The crystalloid was

obtained by recrystallization in petroleum ether (PE), ethanol (EtOH), and water (H₂O). Chiral menthyl ethers **4c** and **4g** were synthesized by performing one recrystallization in PE/EtOH/H₂O, while chiral borneol ether **4h** was obtained through multiple recrystallization in EtOH/H₂O. An enantiomeric mixture of **4d** was obtained in a ratio of 3:1 ($\alpha:\beta \approx 3:1$) in the same manner. However, only the racemates of **4e** and **4f** were obtained by recrystallization.

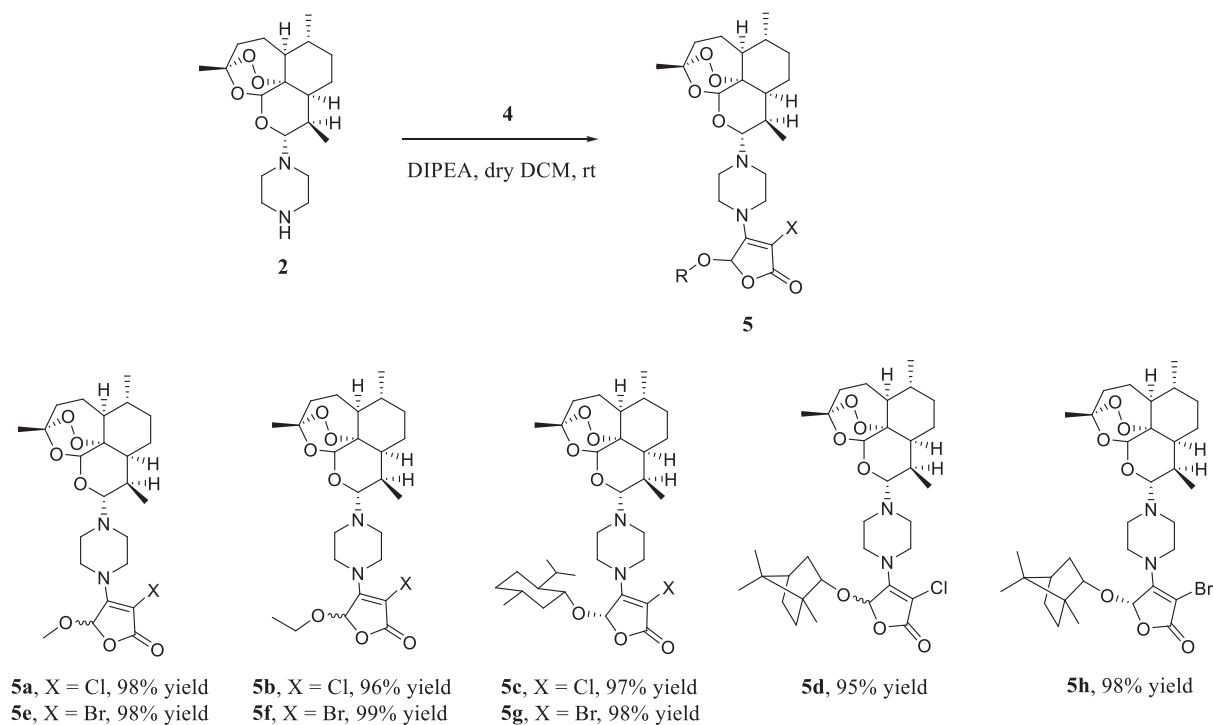
Compound **2** was not as stable as expected and needed to be kept in the refrigerator and avoid thermal reaction. Despite this, the reaction of **2** with furan ethers **4** is nice, and the yield is almost quantitative (>95% yield) at room temperature (Scheme 3). Hybrids **5a–h** was obtained in a simple way. Briefly, a mixture of compound **2**, furan ethers **4**, and *N,N*-diisopropylethylamine (DIPEA) in dichloromethane (DCM) was stirred for 2–4 h at room temperature. We obtained the single crystal of **5c** by dissolving it in dilute hydrochloric acid and ethanol, and its structure was corroborated by X-ray diffraction, as shown in Fig. 2.

2.2. Biological activity of the hybrids

Considering that artemisinin can target the liver, all hybrids including **5a–h**, DHA, VCR and ARA were screened for cytotoxic activity against human hepatocarcinoma cells SMMC-7721 and human normal liver cells LO2 using the standard MTT assay *in vitro*. The results are shown in Table 1. Comparison of the results showed the inhibitory activity of **5a** ($IC_{50} = 0.26 \pm 0.03 \mu\text{M}$ after 24 h) was better than ARA ($IC_{50} = 0.63 \pm 0.04 \mu\text{M}$) and VCR ($IC_{50} = 0.27 \pm 0.03 \mu\text{M}$) *in vitro* against human hepatocarcinoma cells SMMC-7721. Hybrid **5a** ($IC_{50} = 0.32 \pm 0.03 \mu\text{M}$ after 24 h) also had lower cytotoxicity against benign cells LO2 than VCR ($IC_{50} = 0.30 \pm 0.02 \mu\text{M}$ after 24 h). Hybrids **5b**



Scheme 2. Synthesis of furan ethers **4a–h**. Reagents and conditions: (a) MeOH or EtOH, 1,2-dichloroethane, H₂SO₄, rt then reflux; (b) menthol or borneol, cyclohexane, H₂SO₄, rt then reflux.



Scheme 3. Synthesis of novel hybrids 5a–h.

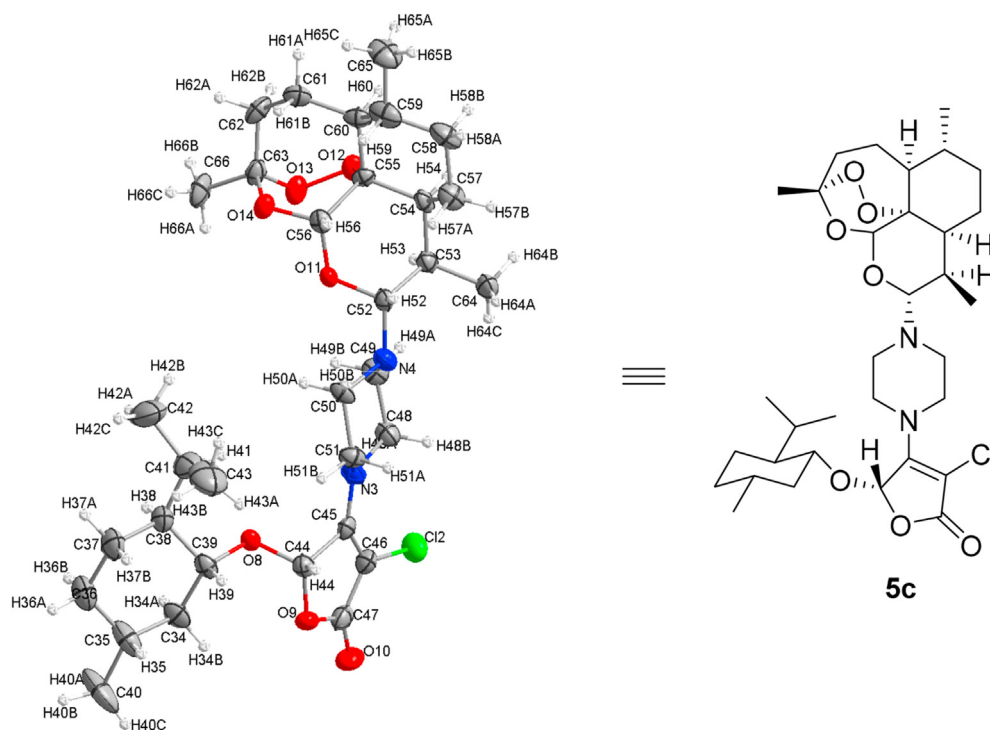


Fig. 2. X-ray structure of hybrid **5c**. Crystallographic data for hybrid **5c** is available from the Cambridge Crystallographic Data Centre under reference number CCDC 2012573. The thermal ellipsoids of all non-hydrogen atoms are shown at 30% probability.

($IC_{50} = 0.70 \pm 0.04 \mu\text{M}$ after 24 h) and **5c** ($IC_{50} = 0.64 \pm 0.03 \mu\text{M}$ after 24 h) had less cytotoxic activity against benign cells LO2 than VCR, ARA, and DHA, although their inhibitory activity against human hepatocarcinoma cells SMMC-7721 was not the best. Considering this, a drug with moderate anti-tumour properties and low

toxicity could be used as an anti-tumour drug by controlling the dosage.

SMMC-7721 = human hepatocarcinoma cells; LO2 = human normal liver cells; VCR = vincristine; ARA = cytosine arabinoside; $\mu\text{M} = \mu\text{mol}/\text{mL}$. IC_{50} values represent the compound concentration

Table 1
Cytotoxic activities against SMMC-7721 and LO2 cells for **5a–h**, VCR, ARA and DHA.

Compound	IC ₅₀ (μM)/24 h	
	SMMC-7721	LO2
5a	0.26 ± 0.03	0.32 ± 0.03
5b	0.56 ± 0.03	0.70 ± 0.04
5c	0.52 ± 0.05	0.64 ± 0.03
5d	0.57 ± 0.03	0.46 ± 0.04
5e	0.29 ± 0.04	0.26 ± 0.03
5f	0.43 ± 0.04	0.50 ± 0.03
5g	0.39 ± 0.04	0.36 ± 0.04
5h	0.48 ± 0.03	0.48 ± 0.01
VCR	0.27 ± 0.03	0.30 ± 0.02
ARA	0.63 ± 0.04	0.43 ± 0.04
DHA	>0.7	0.22 ± 0.04

(μM) required to inhibit tumour cell proliferation by 50% and were calculated using concentrations from triplicate measurements.

As can be seen in Fig. 3, Hybrid **5a** showed the best inhibitory activity against human hepatocarcinoma cells SMMC-7721, and the inhibitory rate increased with increasing concentration. As shown in Fig. 4, the annexin V-FITC (AV) and propidium iodide (PI) staining were used and performed on flow cytometry to explore the apoptotic cells mediated by **5a**. SMMC-7721 cells were treated with **5a** at different concentrations of 0.1, 10, and 100 μg/mL, respectively. As can be seen from Fig. 4, the percentage of early and late apoptotic cells increased (lower right quadrant and upper right quadrant, respectively) as the concentration of hybrid **5a** increased. The average cell apoptosis including the percentage of early and late apoptotic cells, across three parallel experiments, reached to

36.98% when the concentration of hybrid **5a** was 100 μg/mL. It was found that hybrid **5a** could induce the apoptosis of SMMC-7721 cells in a concentration-dependent manner. The results indicated that the antiproliferative effect of **5a** might be related to the induction of apoptosis.

We chose hybrid **5a** to test anti-tumour activity against other cancer cells (Table 2). Hybrid **5a** had good activity against human breast cancer cells MCF-7 (IC₅₀ = 0.08 ± 0.03 μM) after 48 h *in vitro*. The cytotoxic activity of hybrid **5a** against hepatocarcinoma cells SMMC-7721 significantly improved as time progressed, IC₅₀ from 0.26 ± 0.03 μM (Table 1) to 0.11 ± 0.04 μM (Table 2) after 24 h and 48 h, respectively. Studies have shown that some cancer cells can import Fe²⁺ through abnormal iron transporters in their membranes, while normal cells seldom have abnormal iron transporters [26,27]. We tested the cytotoxic activity of hybrid **5a** against human hepatocarcinoma cells SMMC-7721, MHCC97H, and HCCLM3 in the presence of FeSO₄ for 48 h *in vitro*. Instead of directly using the medium containing Fe²⁺ and **5a**, Fe²⁺ was added when culturing cells, which is a good way to simulate the process of cancer cells absorbing Fe²⁺. Hybrid **5a** showed similar activity against human hepatocarcinoma cells with or without Fe²⁺. In our opinion, the anti-tumour mechanism induced by Fe²⁺ remains unclear. The morphological changes of cells induced by hybrid **5a** are shown in Fig. 5. Hybrid **5a** can effectively inhibit the proliferation of tumour cells *in vitro*.

SMMC-7721, MHCC97H, HCCLM3, HUH-7 = human hepatocarcinoma cells. HCT116 = human colon cancer cells. CCD18CO = human normal colon cells. MCF-7 = human breast cancer cells. MCF-10A = human normal breast cells. μM = μmol/mL. IC₅₀ values represent the compound concentration (μM) required to

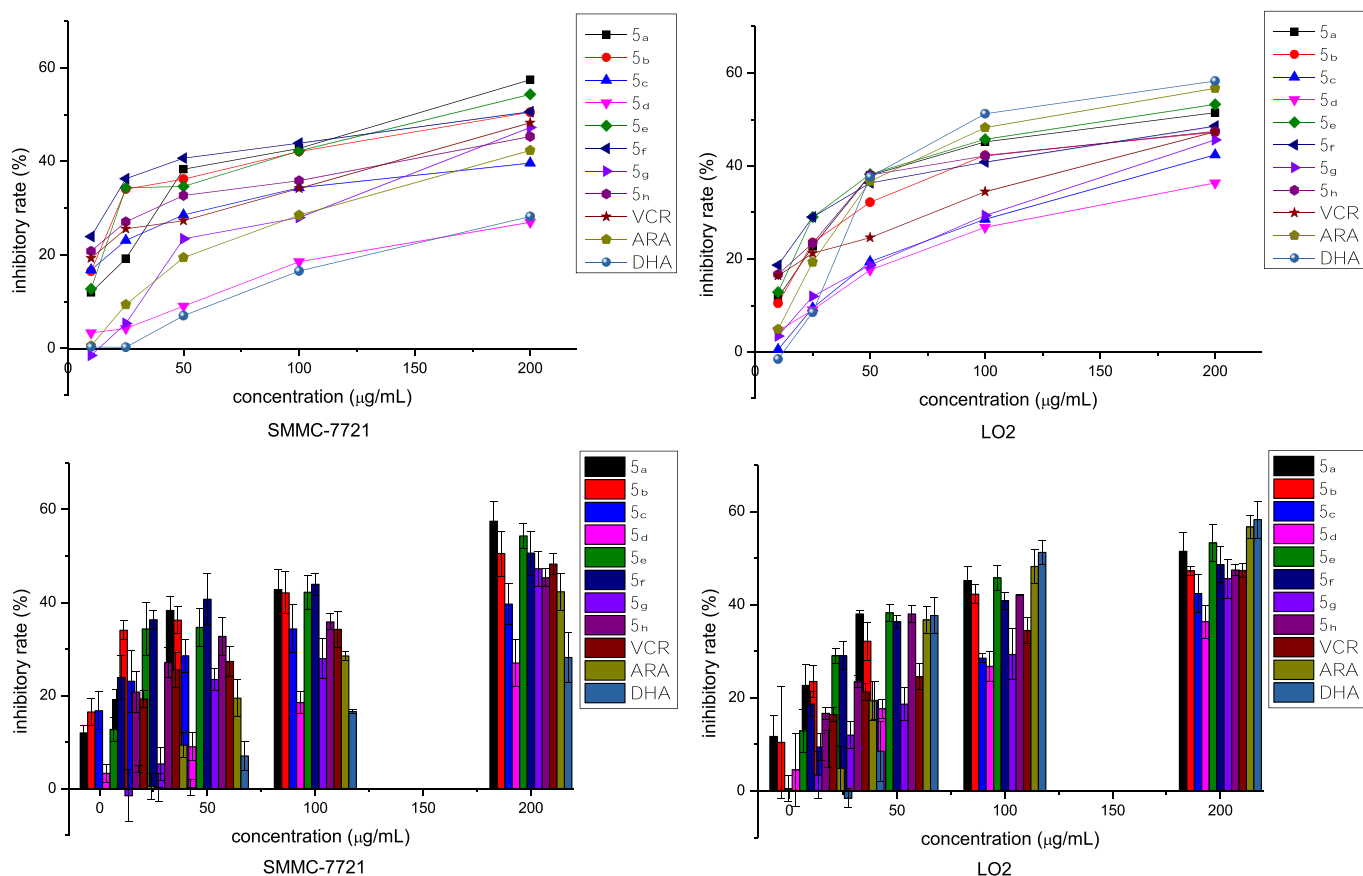


Fig. 3. Inhibitory effect of **5a–h**, VCR, ARA and DHA with various concentrations on SMMC-7721 and LO2 cells for 24 h.

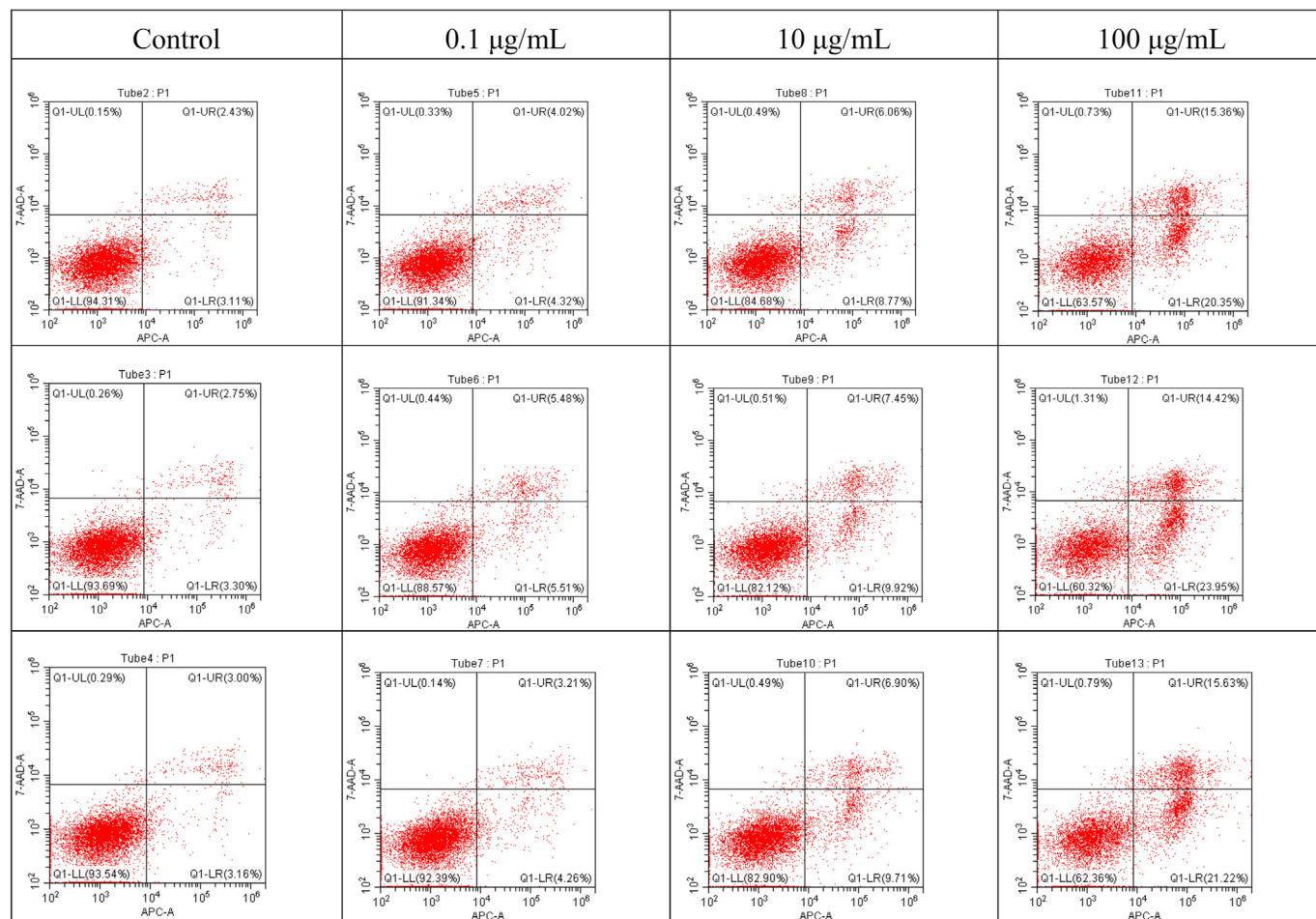


Fig. 4. Flow cytometric analysis of SMMC-7721 cells using different concentrations of hybrid **5a** (0.1, 10, and 100 $\mu\text{g/mL}$); each concentration was detected three times in parallel. The percentage of cells positive for AV and/or PI was reported in the quadrants including cells in the lower left quadrant (live cells), lower right quadrant (early apoptotic cells), upper right quadrant (late apoptotic cells), and upper left quadrant (necrotic cells).

Table 2
Cytotoxic activities of **5a** against cancer and benign cells.

Cells	IC ₅₀ (μM)/48 h
SMMC-7721	0.11 \pm 0.04
SMMC-7721	0.10 \pm 0.04 ^a
MHCC97H	0.10 \pm 0.04
MHCC97H	0.09 \pm 0.05 ^a
HCCLM3	0.10 \pm 0.03
HCCLM3	0.08 \pm 0.03 ^a
HUH-7	0.16 \pm 0.03
HCT116	0.10 \pm 0.03
CCD18CO	0.10 \pm 0.03
MCF-7	0.08 \pm 0.03
MCF-10A	0.22 \pm 0.04

^a Cancer cells were cultured with 100 $\mu\text{mol/L}$ FeSO₄.

inhibit tumour cell proliferation by 50% and were calculated using concentrations from triplicate measurements.

3. Conclusion

For the first time, a series of artemisinin-piperazine-furan ether hybrids were synthesized efficiently, and the absolute configuration of hybrid **5c** was determined by X-ray crystallographic analysis. The cytotoxic activities of the hybrids are presented in this article. Hybrid **5a** showed higher inhibitory activity against human

hepatocarcinoma cells SMMC-7721 than the parent DHA, and two references (VCR and ARA). Hybrid **5a** also had good cytotoxicity against human breast cancer cells MCF-7, and low cytotoxicity against human breast benign cells MCF-10A *in vitro*. Hybrid **5a** also has good activity against other hepatocarcinoma cells (MHCC97H, HCCLM3, HUH-7) *in vitro*. We find that the mechanism of anti-tumour induced by iron ion was not quite explanation. Iron ion can't increase the cytotoxic activity of hybrid **5a**. The results could provide a useful reference for research involving anti-tumour drugs.

4. Experimental

4.1. Synthesis and characterization

4.1.1. General

All starting materials and reagents were purchased from commercially available sources and used without further purification, unless otherwise indicated. ¹H NMR spectra were recorded on a Bruker Avance III 400 MHz spectrometer. Chemical shifts (in ppm) were calibrated with CDCl₃. ¹³C NMR spectra were obtained by using the same NMR spectrometer and were calibrated with CDCl₃. Infrared (IR) spectra of compounds dispersed in potassium bromide were recorded using a Spectrum Two spectrometer, and values are reported as ν in cm⁻¹. High-resolution mass spectrum (HRMS) of

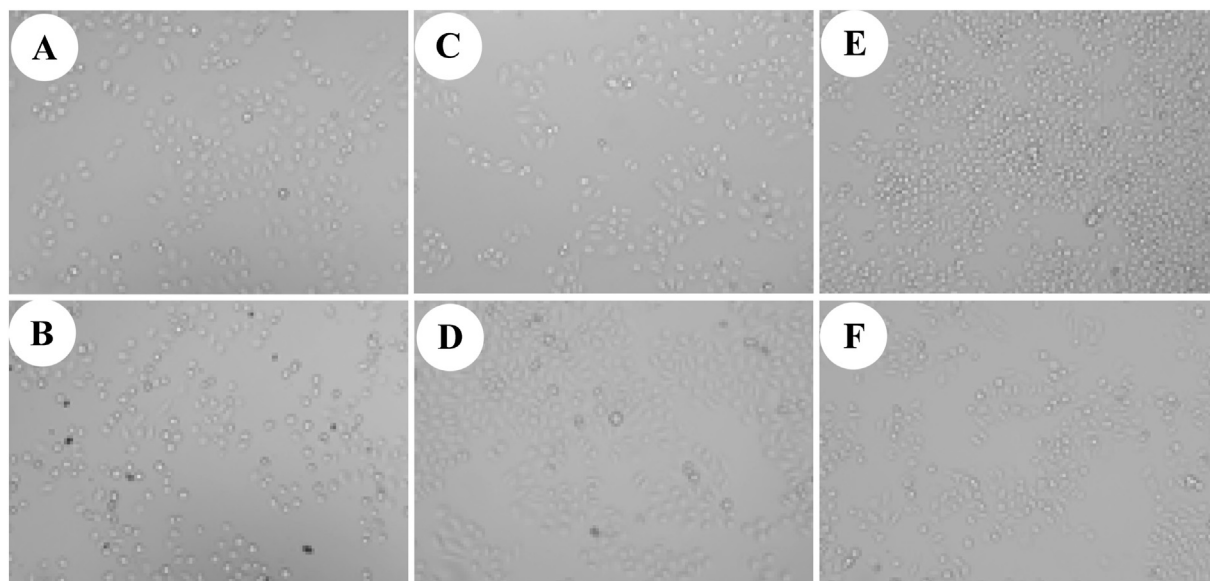


Fig. 5. Morphological changes of cells induced by hybrid **5a** at a concentration of 25 µg/mL after 48 h in (A) SMMC-7721 cells, (B) SMMC-7721 cells with Fe²⁺, (C) MHCC97H cells, (D) MHCC97H cells with Fe²⁺, (E) HCLLM3 cells, and (F) HCLLM3 cells with Fe²⁺.

compounds were recorded on a Thermo Fisher LTQ Orbitrap XL. The X-ray single-crystal data for the compound **5c** was collected on a Bruker AXS SMART 1000 CCD diffractometer using graphite monochromated Mo K α radiation ($\lambda = 0.71073$ Å). The biological activity tests were performed by Wuhan Bafeier Biotechnology Service Co., Ltd.

4.1.2. Synthesis of 1-((3R,5aS,6R,8aS,9R,10R,12aR)-3,6,9-trimethyldecahydro-3H-3,12-epoxy[1,2]dioxepino[4,3-*i*]isochromen-10-yl)piperazine (**2**)

Under the anhydrous condition, anhydrous piperazine (2.5 g, 29 mmol) and dry dichloromethane (DCM) (35 mL) were added to a flask-3-neck (250 mL), then stirred until completely dissolved. Under the anhydrous condition, dry DCM (25 mL) and DHA (2 g, 7 mmol) were added to another flask-3-neck (200 mL) and stirred at room temperature, within 1 min, DMSO (50–80 µL) were added and stirred for another 3 min. Oxalyl chloride (0.6–0.7 mL) was slowly added until no gas was produced and stirred another 7–10 min. The mixture was slowly dropwise in the flask containing piperazine, allowing overnight reaction at room temperature. Following the addition of saturated sodium carbonate (20 mL) and AcOEt (30 mL), the organic phase was separated, and the aqueous layer was extracted with AcOEt (2 × 30 mL). The combined extracts were washed with brine (20 mL), dried over anhydrous Na₂SO₄, and concentrated under reduced pressure. The residue was purified by chromatography on an ammonia-treated silica gel column. Get the elution with 25:1 DCM-methanol. Compound **2** [30] was formed in 68% yield as a yellow solid. m.p. 76.1–76.5 °C; $[\alpha]_D^{20} +19$ (c 2.0, CHCl₃); ¹H NMR (400 MHz, Chloroform-*d*) δ 5.26 (s, 1H), 3.96 (d, *J* = 10.2 Hz, 1H), 2.90 (d, *J* = 17.8 Hz, 6H), 2.57 (ddd, *J* = 10.1, 7.3, 4.3 Hz, 3H), 2.33 (ddd, *J* = 14.5, 13.3, 4.0 Hz, 1H), 2.05–1.94 (m, 1H), 1.72–1.64 (m, 2H), 1.56–1.45 (m, 2H), 1.38 (s, 3H), 1.32–1.27 (m, 2H), 1.21 (td, *J* = 11.2, 6.5 Hz, 1H), 1.07–0.97 (m, 1H), 0.93 (d, *J* = 6.3 Hz, 3H), 0.79 (d, *J* = 7.2 Hz, 3H); ¹³C NMR (101 MHz, CDCl₃) δ 103.8, 91.6, 90.9, 80.3, 51.6, 50.4, 48.3, 46.0, 45.7, 37.3, 36.2, 34.2, 28.2, 25.9, 24.7, 21.6, 20.2, 13.4.

4.1.3. General procedure for the furan ethers **4a–h**

Method A (for **4a**, **4b**, **4e** and **4f**): mucochloric acid or

mucochloric acid **3** (30 mmol), methyl alcohol or ethyl alcohol (1 mL every 8 h), and 1,2-dichloroethane (90 mL) were added to a flask and stirred for 10 min, then 0.5 mL concentrated sulphuric acid added dropwise and stirred for another 20 min. Then a water segregator was set up and heated to reflux for 36 h. After the mixture was cooled to room temperature, saturated sodium carbonate (2 × 40 mL) and saturated salt water (40 mL) were used to wash the mixture, then dried over Na₂SO₄ and the solvent removed under diminished pressure. The residue was purified by chromatography on a silica gel column to give product **4**.

Method B (for **4c**, **4d**, **4g** and **4h**): mucochloric acid or mucochloric acid **3** (30 mmol), menthol (4.68 g, 30 mmol), or borneol (4.63 g, 30 mmol) and cyclohexane (120 mL) were added to a flask and stirred for 10 min, then 0.5 mL concentrated sulphuric acid added dropwise and stirred for another 20 min. Then a water segregator was set up and heated to reflux for 36 h. After the mixture was cooled to room temperature, saturated sodium carbonate (2 × 40 mL), and saturated salt water (40 mL) were used to wash the mixture, then dried over Na₂SO₄ and the solvent removed under diminished pressure. The residue was recrystallised to give product **4**.

4.1.3.1. 3,4-Dichloro-5-methoxyfuran-2(5H)-one (**4a**). Compound **4a** [31,32] was formed in 90% as a colourless oil. ¹H NMR (400 MHz, Chloroform-*d*) δ 5.77 (s, 1H), 3.59 (s, 3H); ¹³C NMR (101 MHz, CDCl₃) δ 163.1, 147.2, 124.5, 101.4, 56.4.

4.1.3.2. 3,4-Dichloro-5-ethoxyfuran-2(5H)-one (**4b**). Compound **4b** [31] was formed in 85% as a colourless oil. ¹H NMR (400 MHz, Chloroform-*d*) δ 5.81 (s, 1H), 3.86 (ddq, *J* = 44.2, 9.3, 7.1 Hz, 2H), 1.31 (t, *J* = 7.1 Hz, 3H); ¹³C NMR (101 MHz, CDCl₃) δ 163.3, 147.4, 124.2, 100.8, 66.1, 14.8.

4.1.3.3. 3,4-Dibromo-5-methoxyfuran-2(5H)-one (**4e**). Compound **4e** [32] was formed in 80% as a colourless solid. m.p. 51.1–51.5 °C; ¹H NMR (400 MHz, Chloroform-*d*) δ 5.78 (s, 1H), 3.58 (s, 3H); ¹³C NMR (101 MHz, CDCl₃) δ 163.9, 142.9, 119.0, 103.7, 56.1.

4.1.3.4. 3,4-Dibromo-5-ethoxyfuran-2(5H)-one (**4f**). Compound **4f**

was formed in 78% as a faint yellow solid. m.p. 40.3–41.0 °C; ^1H NMR (400 MHz, Chloroform-*d*) δ 5.82 (s, 1H), 3.90 (dq, J = 9.4, 7.1 Hz, 1H), 3.80 (dq, J = 9.4, 7.1 Hz, 1H), 1.32 (t, J = 7.1 Hz, 3H); ^{13}C NMR (101 MHz, CDCl_3) δ 164.1, 143.2, 118.7, 103.1, 65.9, 14.9.

4.1.3.5. (*S*)-3,4-Dichloro-5-(((1*S*,2*S*,5*R*)-2-isopropyl-5-methylcyclohexyl)oxy)furan-2(5*H*)-one (**4c**). Compound **4c** [33] was crystallized from EtOH/PE/H₂O in 31% as a colourless crystal. m.p. 112.4–113.4 °C; $[\alpha]_{\text{D}}^{20}$ +53 (c 1.0, CHCl_3); ^1H NMR (400 MHz, Chloroform-*d*) δ 5.85 (d, J = 31.3 Hz, 1H), 3.63 (dtd, J = 34.2, 10.7, 4.4 Hz, 1H), 2.30–2.06 (m, 2H), 1.68 (dh, J = 10.5, 2.7, 2.3 Hz, 2H), 1.57 (s, 1H), 1.46–1.27 (m, 1H), 1.11–1.02 (m, 1H), 0.97 (d, J = 6.6 Hz, 2H), 0.93 (dd, J = 6.8, 3.7 Hz, 2H), 0.89 (d, J = 7.1 Hz, 3H), 0.82–0.77 (m, 3H); ^{13}C NMR (101 MHz, CDCl_3) δ 163.4, 147.6, 123.9, 102.2, 84.5, 47.9, 42.1, 33.9, 31.6, 25.3, 22.9, 22.0, 20.8, 15.8.

4.1.3.6. 3,4-Dichloro-5-(((2*S*)-1,7,7-trimethylbicyclo[2.2.1]heptan-2-yl)oxy)furan-2(5*H*)-one (**4d**). Compound **4d** [34] was crystallized from EtOH/H₂O in 33% as a white crystal. m.p. 79.8–80.2 °C; $[\alpha]_{\text{D}}^{20}$ –15 (c 1.0, CHCl_3); ^1H NMR (400 MHz, Chloroform-*d*) δ 5.80 (d, J = 9.5 Hz, 1H), 4.06 (dddd, J = 37.4, 9.9, 3.3, 1.9 Hz, 1H), 3.69 (dp, J = 20.0, 6.8 Hz, 1H), 3.08 (q, J = 7.4 Hz, 1H), 2.33–2.18 (m, 1H), 1.92 (ddd, J = 14.0, 10.0, 4.3 Hz, 1H), 1.81–1.56 (m, 6H), 1.52–1.37 (m, 3H), 1.33–1.21 (m, 3H), 0.93 (s, 2H), 0.90–0.84 (m, 9H); ^{13}C NMR (101 MHz, CDCl_3) δ 163.4, 147.6, 124.1, 102.4, 100.5, 89.1, 86.1, 49.8, 49.4, 48.1, 47.7, 44.9, 44.8, 36.6, 36.1, 28.1, 27.9, 26.5, 26.3, 19.6 (\times 2), 18.8, 18.7, 13.6, 13.3.

4.1.3.7. (*S*)-3,4-Dibromo-5-(((1*R*,2*S*,5*R*)-2-isopropyl-5-methylcyclohexyl)oxy)furan-2(5*H*)-one (**4g**). Compound **4g** [35] was crystallized from EtOH/PE/H₂O in 35% as a gray crystal. m.p. 140.2–140.8 °C; $[\alpha]_{\text{D}}^{20}$ +37 (c 1.0, CHCl_3); ^1H NMR (400 MHz, Chloroform-*d*) δ 5.81 (s, 1H), 3.59 (td, J = 10.7, 4.4 Hz, 1H), 2.32 (qt, J = 7.0, 3.5 Hz, 1H), 2.29–2.21 (m, 1H), 1.74–1.63 (m, 2H), 1.56 (s, 4H), 1.46–1.38 (m, 1H), 1.38–1.32 (m, 1H), 1.11 (td, J = 12.4, 11.0 Hz, 1H), 1.04–0.98 (m, 1H), 0.94 (dd, J = 6.8, 2.3 Hz, 6H), 0.90–0.86 (m, 1H), 0.82 (d, J = 6.9 Hz, 3H); ^{13}C NMR (101 MHz, CDCl_3) δ 164.3, 143.4, 118.5, 104.5, 84.5, 77.2, 58.5, 48.0, 42.1, 33.9, 31.6, 25.2, 22.8, 22.1, 20.9, 18.4, 15.8.

4.1.3.8. (5*S*)-3,4-Dibromo-5-(((2*S*)-1,7,7-trimethylbicyclo[2.2.1]heptan-2-yl)oxy)furan-2(5*H*)-one (**4h**). Compound **4h** [34] was crystallized from EtOH/H₂O in 14% as a colourless crystal. m.p. 95.0–95.6 °C; $[\alpha]_{\text{D}}^{20}$ +8 (c 1.0, CHCl_3); ^1H NMR (400 MHz, Chloroform-*d*) δ 5.78 (d, J = 1.3 Hz, 1H), 3.74 (ddd, J = 31.8, 7.8, 3.4 Hz, 1H), 1.96 (ddq, J = 20.9, 13.3, 3.6 Hz, 1H), 1.82–1.76 (m, 1H), 1.76–1.71 (m, 1H), 1.71–1.63 (m, 1H), 1.55 (s, 2H), 1.08–1.00 (m, 3H), 1.00–0.92 (m, 5H), 0.91–0.82 (m, 6H), 0.81–0.71 (m, 1H); ^{13}C NMR (101 MHz, CDCl_3) δ 164.3, 143.7, 104.5, 102.1, 90.3, 87.6, 49.9, 49.2, 46.7, 46.7, 45.0, 39.3, 38.5, 34.0, 27.0, 20.0, 12.0, 11.7.

4.1.4. General procedure for the hybrids **5a–h**

Compound **2** (40 mg, 0.14 mmol), furan ethers **4** (0.14 mmol), DIPEA (0.2 mL) and DCM (15 mL) were added to a flask, and stirred for 2–4 h at room temperature. The reaction mixture was evaporated under reduced pressure and the residue was purified by chromatography on a silica gel column (5–6 cm, 20:1 to 5:1 petroleum ether–ethyl acetate) to give hybrids **5a–h**.

4.1.4.1. 3-Chloro-5-methoxy-4-(4-((3*R*,5*aS*,6*R*,8*aS*,9*R*,10*R*,12*aR*)-3,6,9-trimethyldecahydro-3*H*-3,12-epoxy[1,2]dioxepino[4,3-*i*]isochromen-10-yl)piperazin-1-yl)furan-2(5*H*)-one (**5a**). Hybrid **5a** was formed in 98% as a yellow solid. m.p. 93.3–94.0 °C; $[\alpha]_{\text{D}}^{20}$ +8 (c 1.0,

CHCl_3); ^1H NMR (400 MHz, Chloroform-*d*) δ 5.69 (d, J = 2.5 Hz, 1H), 5.28 (s, 1H), 4.03 (dd, J = 10.3, 3.3 Hz, 1H), 3.85 (s, 1H), 3.70 (s, 4H), 3.47 (d, J = 4.9 Hz, 3H), 3.14–2.99 (m, 2H), 2.81–2.71 (m, 2H), 2.34 (td, J = 14.0, 3.7 Hz, 1H), 2.03–1.97 (m, 1H), 1.87 (dq, J = 10.2, 3.3 Hz, 1H), 1.71 (dq, J = 10.7, 3.5 Hz, 2H), 1.60 (s, 3H), 1.58–1.44 (m, 1H), 1.39 (d, J = 1.6 Hz, 3H), 1.35 (s, 1H), 1.07–0.99 (m, 1H), 0.95 (d, J = 6.2 Hz, 3H), 0.82 (d, J = 7.1 Hz, 3H); ^{13}C NMR (101 MHz, CDCl_3) δ 168.3, 153.8, 104.1, 97.5, 91.8, 90.7, 86.7, 80.4, 54.5, 54.3, 51.8, 45.8, 37.5, 36.4, 34.4, 28.5, 26.1, 26.1, 24.9, 21.8, 20.4, 13.6; IR (KBr) ν/cm^{-1} : 3455, 2928, 1763, 1635, 1449, 1207, 1122, 983, 880, 745; HRMS m/z : calcd for $\text{C}_{24}\text{H}_{35}\text{ClN}_2\text{O}_7\text{Na}$ 521.2025, found 521.2001 $[\text{M}+\text{Na}]^+$.

4.1.4.2. 3-Chloro-5-ethoxy-4-(4-((3*R*,5*aS*,6*R*,8*aS*,9*R*,10*R*,12*aR*)-3,6,9-trimethyldecahydro-3*H*-3,12-epoxy[1,2]dioxepino[4,3-*i*]isochromen-10-yl)piperazin-1-yl)furan-2(5*H*)-one (**5b**). Compound **5b** was formed in 96% as a yellow solid. m.p. 67.0–68.0 °C; $[\alpha]_{\text{D}}^{20}$ –4 (c 1.0, CH_3OH); ^1H NMR (400 MHz, Chloroform-*d*) δ 5.71 (d, J = 3.4 Hz, 1H), 5.27 (d, J = 8.9 Hz, 1H), 4.02 (dd, J = 10.3, 4.3 Hz, 1H), 3.85–3.61 (m, 4H), 3.05 (td, J = 10.4, 4.8 Hz, 2H), 2.81–2.66 (m, 2H), 2.58–2.52 (m, 1H), 2.32 (td, J = 14.1, 3.9 Hz, 1H), 2.02–1.96 (m, 1H), 1.85 (ddt, J = 13.4, 6.7, 3.6 Hz, 1H), 1.77–1.66 (m, 2H), 1.53 (ddt, J = 11.7, 7.6, 4.4 Hz, 1H), 1.38–1.31 (m, 4H), 1.29–1.20 (m, 8H), 1.02–0.97 (m, 1H), 0.93 (d, J = 6.2 Hz, 3H), 0.80 (d, J = 7.0 Hz, 3H); ^{13}C NMR (101 MHz, CDCl_3) δ 168.4, 154.1, 104.2, 96.9, 91.7, 90.7, 86.6, 80.4, 64.1, 63.7, 51.8, 45.8, 37.5, 36.4, 34.3, 28.5, 28.4, 26.1, 24.9, 21.8, 20.4, 15.1, 13.6; IR (KBr) ν/cm^{-1} : 2929, 2873, 1763, 1636, 1449, 1258, 1131, 978, 880, 745; HRMS m/z : calcd for $\text{C}_{25}\text{H}_{37}\text{ClN}_2\text{O}_7\text{Na}$ 535.2182, found 535.2156 $[\text{M}+\text{Na}]^+$.

4.1.4.3. (5*S*)-3-chloro-5-(((1*S*,2*R*,5*S*)-2-isopropyl-5-methylcyclohexyl)oxy)-4-(4-((3*R*,5*aS*,6*R*,8*aS*,9*R*,10*R*,12*aR*)-3,6,9-trimethyldecahydro-3*H*-3,12-epoxy[1,2]dioxepino[4,3-*i*]isochromen-10-yl)piperazin-1-yl)furan-2(5*H*)-one (**5c**). Compound **5c** was formed in 97% as a yellow solid. m.p. 101.3–102.0 °C; $[\alpha]_{\text{D}}^{20}$ –24 (c 1.0, CH_3OH); ^1H NMR (400 MHz, Chloroform-*d*) δ 5.77 (s, 1H), 5.28 (s, 1H), 4.02 (d, J = 10.3 Hz, 1H), 3.78 (s, 2H), 3.55 (dd, J = 15.6, 4.9 Hz, 2H), 3.11–3.03 (m, 2H), 2.78–2.70 (m, 2H), 2.56 (ddd, J = 10.8, 7.2, 4.4 Hz, 1H), 2.39–2.29 (m, 1H), 2.25–2.14 (m, 2H), 2.04–1.83 (m, 2H), 1.76–1.27 (m, 14H), 1.23–0.98 (m, 3H), 0.96–0.90 (m, 11H), 0.82 (d, J = 7.1 Hz, 3H), 0.76 (d, J = 6.9 Hz, 3H); ^{13}C NMR (101 MHz, CDCl_3) δ 168.5, 155.1, 104.2, 97.2, 91.7, 90.7, 87.2, 80.7, 80.4, 51.8, 48.3, 48.2, 45.8, 42.6, 37.5, 36.4, 34.4, 34.1, 31.8, 28.5, 26.1, 25.2, 24.9, 22.9, 22.4, 21.8, 21.3, 20.4, 15.9, 14.3, 13.6; IR (KBr) ν/cm^{-1} : 2928, 2871, 1763, 1634, 1449, 1257, 1119, 973, 880, 746; HRMS m/z : calcd for $\text{C}_{33}\text{H}_{52}\text{ClN}_2\text{O}_7$ 623.3458, found 623.3436 $[\text{M}+\text{H}]^+$.

4.1.4.4. 3-Chloro-5-(((2*S*)-1,7,7-trimethylbicyclo[2.2.1]heptan-2-yl)oxy)-4-(4-((3*R*,5*aS*,6*R*,8*aS*,9*R*,10*R*,12*aR*)-3,6,9-trimethyldecahydro-3*H*-3,12-epoxy[1,2]dioxepino[4,3-*i*]isochromen-10-yl)piperazin-1-yl)furan-2(5*H*)-one (**5d**). Compound **5d** was formed in 95% as a yellow solid. m.p. 111.0–112.0 °C; $[\alpha]_{\text{D}}^{20}$ –6 (c 1.0, CH_3OH); ^1H NMR (400 MHz, Chloroform-*d*) δ 5.72–5.63 (m, 1H), 5.28 (d, J = 1.9 Hz, 1H), 4.02 (d, J = 10.2 Hz, 1H), 3.82–3.68 (m, 3H), 3.59 (dd, J = 12.2, 9.4 Hz, 2H), 3.06 (q, J = 10.8, 9.1 Hz, 3H), 2.77 (dt, J = 15.5, 7.9 Hz, 3H), 2.63–2.51 (m, 1H), 2.34 (td, J = 14.0, 3.9 Hz, 1H), 2.03–1.98 (m, 1H), 1.90–1.82 (m, 2H), 1.74–1.66 (m, 4H), 1.54 (dq, J = 10.0, 5.3, 4.7 Hz, 1H), 1.47–1.31 (m, 5H), 1.01 (q, J = 7.0, 5.9 Hz, 3H), 0.97–0.93 (m, 7H), 0.91–0.86 (m, 3H), 0.81 (td, J = 7.0, 6.6, 2.6 Hz, 7H); ^{13}C NMR (101 MHz, CDCl_3) δ 168.5, 154.8, 104.1, 98.4, 96.2, 91.6, 90.6, 88.6, 86.1, 80.3, 51.7, 49.6, 49.3, 46.8, 45.8, 45.2, 39.9, 37.4, 36.3, 34.6, 34.3, 28.4, 27.1, 26.1, 24.8, 21.7, 20.3, 20.2, 13.5, 12.5, 12.0; IR (KBr) ν/cm^{-1} : 2953, 2873, 1766, 1635, 1453, 1121, 974, 880, 745; HRMS m/z : calcd for $\text{C}_{33}\text{H}_{49}\text{ClN}_2\text{O}_7\text{Na}$ 643.3121, found 643.3091 $[\text{M}+\text{Na}]^+$.

4.1.4.5. *3-Bromo-5-methoxy-4-(4-((3R,5aS,6R,8aS,9R,10R,12aR)-3,6,9-trimethyldecahydro-3H-3,12-epoxy[1,2]dioxepino[4,3-i]isochromen-10-yl)piperazin-1-yl)furan-2(5H)-one (5e)*. Compound **5e** was formed in 98% as a yellow solid. m.p. 88.6–89.4 °C; $[\alpha]_D^{20} -5$ (c 1.0, CH₃OH); ¹H NMR (400 MHz, Chloroform-*d*) δ 5.74 (d, *J* = 3.6 Hz, 1H), 5.28 (s, 1H), 4.03 (d, *J* = 10.2 Hz, 1H), 3.87–3.74 (m, 1H), 3.72–3.62 (m, 1H), 3.12–3.02 (m, 1H), 2.82–2.71 (m, 2H), 2.61–2.53 (m, 1H), 2.34 (td, *J* = 13.9, 3.9 Hz, 1H), 2.04–1.98 (m, 2H), 1.91–1.83 (m, 1H), 1.71 (dq, *J* = 10.5, 3.5 Hz, 2H), 1.61 (s, 1H), 1.55 (dt, *J* = 13.8, 4.3 Hz, 1H), 1.39 (d, *J* = 6.6 Hz, 3H), 1.36–1.29 (m, 1H), 1.26 (td, *J* = 7.1, 2.2 Hz, 8H), 0.95 (d, *J* = 6.2 Hz, 3H), 0.83–0.80 (m, 3H); ¹³C NMR (101 MHz, CDCl₃) δ 168.6, 156.7, 104.0, 97.7, 91.6, 90.5, 80.3, 63.9, 63.5, 60.4, 51.7, 45.7, 37.4, 36.3, 34.2, 28.3, 26.0, 24.7, 21.6, 20.3, 15.0, 13.5; IR (KBr) ν/cm^{-1} : 2931, 1761, 1628, 1450, 1257, 1206, 962, 880, 744; HRMS *m/z*: calcd for C₂₄H₃₅BrN₂O₇K 581.1259, found 581.1750 [M+K]⁺.

4.1.4.6. *3-Bromo-5-ethoxy-4-(4-((3R,5aS,6R,8aS,9R,10R,12aR)-3,6,9-trimethyldecahydro-3H-3,12-epoxy[1,2]dioxepino[4,3-i]isochromen-10-yl)piperazin-1-yl)furan-2(5H)-one (5f)*. Compound **5f** was formed in 99% as a yellow solid. m.p. 98.9–99.9 °C; $[\alpha]_D^{20} -5$ (c 1.0, CH₃OH); ¹H NMR (400 MHz, Chloroform-*d*) δ 5.74 (d, *J* = 3.5 Hz, 1H), 5.27 (s, 1H), 4.02 (d, *J* = 10.3 Hz, 1H), 3.87–3.62 (m, 5H), 3.06 (td, *J* = 11.2, 7.1 Hz, 2H), 2.83–2.69 (m, 2H), 2.56 (dddd, *J* = 9.9, 7.0, 4.5, 2.5 Hz, 1H), 2.33 (td, *J* = 14.0, 4.0 Hz, 1H), 2.03–1.95 (m, 1H), 1.86 (ddd, *J* = 13.6, 6.6, 3.3 Hz, 1H), 1.74–1.65 (m, 2H), 1.55 (dt, *J* = 13.6, 4.2 Hz, 1H), 1.49–1.40 (m, 1H), 1.39–1.22 (m, 10H), 1.00 (ddd, *J* = 14.2, 12.5, 9.8 Hz, 1H), 0.94 (d, *J* = 6.2 Hz, 3H), 0.82–0.79 (m, 3H); ¹³C NMR (101 MHz, CDCl₃) δ 168.8, 156.7, 104.2, 97.7, 91.7, 90.7, 80.4, 72.7, 63.9, 63.5, 51.8, 45.8, 37.5, 36.4, 34.3, 28.5, 27.0, 26.1, 24.8, 21.7, 20.4, 15.1, 13.5; IR (KBr) ν/cm^{-1} : 2929, 2872, 1761, 1628, 1449, 1118, 1017, 880, 744; HRMS *m/z*: calcd for C₂₅H₃₈BrN₂O₇ 557.1857, found 557.1860 [M+H]⁺.

4.1.4.7. *(5S)-3-Bromo-5-(((1S,2R,5S)-2-isopropyl-5-methylcyclohexyl)oxy)-4-(4-((3R,5aS,6R,8aS,9R,10R,12aR)-3,6,9-trimethyldecahydro-3H-3,12-epoxy[1,2]dioxepino[4,3-i]isochromen-10-yl)piperazin-1-yl)furan-2(5H)-one (5g)*. Compound **5g** was formed in 98% as a yellow solid. m.p. 101.5–102.8 °C; $[\alpha]_D^{20} -19$ (c 1.0, CH₃OH); ¹H NMR (400 MHz, Chloroform-*d*) δ 5.78 (s, 1H), 5.27 (s, 1H), 4.01 (d, *J* = 10.2 Hz, 1H), 3.82 (s, 2H), 3.71–3.48 (m, 3H), 3.10–3.02 (m, 2H), 2.73 (ddd, *J* = 11.3, 7.3, 3.1 Hz, 2H), 2.58–2.51 (m, 1H), 2.33 (td, *J* = 13.9, 3.8 Hz, 1H), 2.23–2.12 (m, 2H), 2.05–1.94 (m, 1H), 1.86 (ddt, *J* = 13.5, 6.7, 3.6 Hz, 1H), 1.79 (s, 2H), 1.73–1.61 (m, 3H), 1.54 (dt, *J* = 13.8, 4.3 Hz, 1H), 1.48–1.26 (m, 6H), 1.22–0.97 (m, 3H), 0.95–0.89 (m, 11H), 0.89–0.82 (m, 1H), 0.81 (dd, *J* = 7.1, 3.1 Hz, 3H), 0.75 (d, *J* = 7.0 Hz, 3H); ¹³C NMR (101 MHz, CDCl₃) δ 168.9, 157.6, 156.7, 104.2, 98.1, 91.7, 90.6, 80.6, 80.4, 73.6, 72.8, 63.9, 51.8, 48.3, 45.8, 42.6, 37.5, 36.4, 34.4, 31.8, 28.5, 26.1, 24.9, 22.9, 22.4, 21.8, 21.3, 20.4, 15.9, 15.1, 13.5; IR (KBr) ν/cm^{-1} : 2928, 2871, 1761, 1627, 1449, 1118, 961, 880, 744; HRMS *m/z*: calcd for C₃₃H₅₂BrN₂O₇ 667.2952, found 667.2955 [M+H]⁺.

4.1.4.8. *(5S)-3-Bromo-5-(((2S)-1,7,7-trimethylbicyclo[2.2.1]heptan-2-yl)oxy)-4-(4-((3R,5aS,6R,8aS,9R,10R,12aR)-3,6,9-trimethyldecahydro-3H-3,12-epoxy[1,2]dioxepino[4,3-i]isochromen-10-yl)piperazin-1-yl)furan-2(5H)-one (5h)*. Compound **5h** was formed in 98% as a yellow solid. m.p. 113.5–114.6 °C; $[\alpha]_D^{20} -14$ (c 1.0, CH₃OH); ¹H NMR (400 MHz, Chloroform-*d*) δ 5.75–5.67 (m, 1H), 5.26 (d, *J* = 6.6 Hz, 1H), 4.02 (d, *J* = 10.3 Hz, 1H), 3.92 (d, *J* = 8.2 Hz, 1H), 3.71 (d, *J* = 40.6 Hz, 4H), 3.12–3.02 (m, 2H), 2.83–2.71 (m, 2H), 2.62–2.51 (m, 1H), 2.40–2.28 (m, 1H), 2.24 (td, *J* = 10.4, 5.5 Hz, 1H), 2.04–1.95 (m, 2H), 1.92–1.84 (m, 1H), 1.70 (td, *J* = 8.8, 7.7, 3.7 Hz, 4H), 1.64 (t, *J* = 4.6 Hz, 1H), 1.55 (dt, *J* = 13.7, 4.2 Hz, 1H), 1.46 (dd,

J = 12.4, 4.2 Hz, 1H), 1.38 (d, *J* = 10.2 Hz, 4H), 1.31 (t, *J* = 3.8 Hz, 1H), 1.18 (t, *J* = 7.1 Hz, 1H), 1.11–0.98 (m, 2H), 0.94 (d, *J* = 6.5 Hz, 3H), 0.88 (dd, *J* = 6.3, 2.4 Hz, 2H), 0.86 (d, *J* = 1.7 Hz, 3H), 0.84 (d, *J* = 1.7 Hz, 3H), 0.83–0.82 (m, 3H), 0.80 (dd, *J* = 6.2, 3.1 Hz, 2H); ¹³C NMR (101 MHz, CDCl₃) δ 168.9, 157.3, 104.2, 99.3, 91.7, 90.7, 87.1, 80.4, 80.3, 51.8, 49.6, 47.7, 45.8, 45.0, 37.5, 37.3, 36.4, 34.4, 28.5, 28.4, 28.2, 26.8, 26.1, 26.0, 24.9, 21.8, 20.4, 19.8, 19.0, 14.2, 13.6; IR (KBr) ν/cm^{-1} : 2952, 1763, 1628, 1452, 1206, 1127, 962, 880, 744; HRMS *m/z*: calcd for C₃₃H₅₀BrN₂O₇ 665.2796, found 665.2794 [M+H]⁺.

4.2. Pharmacology

4.2.1. Human liver cancer cell lines SMMC-7721

SMMC-7721 cells (1×10^4 in 100 μL) were seeded on 96 plates in triplicate. Following a 24 h culture at 37 °C, the medium was replaced with fresh medium at various concentrations (10, 25, 50, 100, and 200 μg/mL) of compounds **5a–h**, DHA, vincristine (VCR) and cytosine arabinoside (ARA) in a final volume of 100 μL. At the same time, the drug-free medium negative control well and the solvent control well were set with the same volume of dimethyl sulfoxide (DMSO). Cells were respectively incubated at 37 °C for 24 h. Then, 10 μL of 3-(4,5-dime-thylthiazol-2-yl)-2,5-diphenyl tetrazolium bromide (MTT) (2 mg/mL in a phosphate buffer solution (PBS)) was added to each well, incubated for an additional 4 h, centrifuged at 1000 r/min for 10 min, and then the medium was removed. MTT formazan precipitates were dissolved in 150 μL of DMSO, shaken mechanically for 10 min and then read immediately at 568 nm using a plate reader (Multiskan MK3, Thermo Fisher Scientific, USA).

Cell inhibition rate = $[A_{568}(\text{negative control well}) - A_{568}(\text{dosing well})]/A_{568}(\text{negative control well}) \times 100\%$

4.2.2. Human normal liver cell lines LO2

The method was similar to that of SMMC-7721 cells described above.

4.2.3. The general method for testing the activity of compound 5a

Cells (SMMC-7721, MHCC97H, HCCLM3, HUH-7, HCT116, CCD18CO, MCF-7, and MCF-10A) (1×10^4 in 100 μL) were respective seeded on 96 plates in triplicate. Following a 24 h culture at 37 °C, the medium was replaced with fresh medium at various concentrations (0.01, 0.1, 1, 10, and 25 μg/mL) of compound **5a** in a final volume of 100 μL. At the same time, the drug-free medium negative control well and the solvent control well were set with the same volume of dimethyl sulfoxide (DMSO). Cells were respectively incubated at 37 °C for 48 h. Then, 10 μL of 3-(4,5-dime-thylthiazol-2-yl)-2,5-diphenyltetrazolium bromide (MTT) (2 mg/mL in a phosphate buffer solution (PBS)) was added to each well, incubated for an additional 4 h, centrifuged at 1000 r/min for 10 min, and then the medium was removed. MTT formazan precipitates were dissolved in 150 μL of DMSO, shaken mechanically for 10 min and then read immediately at 568 nm using a plate reader (Multiskan MK3, Thermo Fisher Scientific, USA).

Cell inhibition rate = $[A_{568}(\text{negative control well}) - A_{568}(\text{dosing well})]/A_{568}(\text{negative control well}) \times 100\%$

4.2.4. Flow cytometry analysis

SMMC-7721 cells were seeded in on 96 plates in triplicate. Following a 24 h culture at 37 °C, the medium was replaced with

fresh medium at various concentrations (0.1, 10, and 100 $\mu\text{g}/\text{mL}$) of compound **5a**. At the same time, drug-free medium negative control well and solvent control well were set with the same volume of dimethyl sulfoxide (DMSO). Cells were respectively cultivated at 37 $^{\circ}\text{C}$ for 48 h then 0.25% trypsin without ethylene diamine tetra acetic acid (EDTA) was added to each well. After trypsinisation, the treated cells were stained using Annexin V-FITC/PI apoptosis detection kit (Nanjing KeyGen Biotech Co., Ltd, CHN) according to the manufacturer's instructions. After incubation at room temperature for 5–15 min in the dark, the apoptotic cells were immediately analysed by flow cytometry (cyto Flex, BECKMAN COULTER, USA).

4.2.5. The general method for testing the activity of compound **5a** in Fe^{2+} environment

Cells (SMMC-7721, MHCC97H, HCCLM3) (1×10^4 in 100 μL) were respectively seeded on 96 plates in triplicate. Following a 12 h culture at 37 $^{\circ}\text{C}$, add 100 $\mu\text{mol}/\text{L}$ FeSO_4 culture solution and culture other 12 h at 37 $^{\circ}\text{C}$. The medium was replaced with fresh medium at various concentrations (0.01, 0.1, 1, 10, and 25 $\mu\text{g}/\text{mL}$) of compound **5a** in a final volume of 100 μL . At the same time, the drug-free medium negative control well and the solvent control well were set with the same volume of dimethyl sulfoxide (DMSO). Cells were respectively incubated at 37 $^{\circ}\text{C}$ for 48 h. Then, 10 μL of 3-(4,5-dimethylthiazol-2-yl)-2,5-diphenyltetrazolium bromide (MTT) (2 mg/mL in a phosphate buffer solution (PBS)) was added to each well, incubated for an additional 4 h, centrifuged at 1000 r/min for 10 min, and then the medium was removed. MTT formazan precipitates were dissolved in 150 μL of DMSO, shaken mechanically for 10 min and then read immediately at 568 nm using a plate reader (Multiskan MK3, Thermo Fisher Scientific, USA).

Cell inhibition rate = $\frac{[A_{568}(\text{negative control well}) - A_{568}(\text{dosing well})]}{A_{568}(\text{negative control well})} \times 100\%$.

Declaration of competing interest

The authors declare that they have no known competing financial interests or personal relationships that could have appeared to influence the work reported in this paper.

Acknowledgments

We are thankful for the financial support from the National Natural Science Foundation of China (No. 21462032), the Natural Science Foundation of Ningxia (No. 2019AAC03018), the Third Batch of Ningxia Youth Talents Supporting Program (No. TJGC2018100), the Discipline Project of Ningxia (No. NXYLXK2017A04), and the College Students' Innovative and Entrepreneurship Training Program of Ningxia University (No. G2020107490003). Thanks to Wuhan Bafeier Biotechnology Service Co., Ltd. for testing the biological activity.

Appendix A. Supplementary data

Supplementary data to this article can be found online at <https://doi.org/10.1016/j.ejmech.2021.113295>.

References

[1] Y.C. Wu, S.H. Luo, W.J. Mei, L. Cao, H.Q. Wu, Z.Y. Wang, Synthesis and biological evaluation of 4-biphenylamino-5-halo-2(5H)-furanones as potential anticancer agents, *Eur. J. Med. Chem.* 139 (2017) 84–94, <https://doi.org/10.1016/j.ejmech.2017.08.005>.

- [2] C.K. Peng, T. Zeng, X.J. Xu, Y.Q. Chang, W. Hou, K. Lu, H. Lin, P.H. Sun, J. Lin, W.M. Chen, Novel 4-(4-substituted amidobenzyl)furan-2(5H)-one derivatives as topoisomerase I inhibitors, *Eur. J. Med. Chem.* 127 (2017) 187–199, <https://doi.org/10.1016/j.ejmech.2016.12.035>.
- [3] H.R. Khatri, B. Bhattarai, W. Kaplan, Z.Z. Li, M.J.C. Long, Y. Aye, P. Nagorny, Modular total synthesis and cell-based anticancer activity evaluation of ouabagenin and other cardiotonic steroids with varying degrees of oxygenation, *J. Am. Chem. Soc.* 141 (2019) 4849–4860, <https://doi.org/10.1021/jacs.8b12870>.
- [4] F.M. Xi, S.G. Ma, Y.B. Liu, L. Li, S.S. Yu, Artaboterpenoids A and B, bisabolene-derived sesquiterpenoids from *Artabotrys hexapetalus*, *Org. Lett.* 18 (2016) 3374–3377, <https://doi.org/10.1021/acs.orglett.6b01519>.
- [5] S.H. Luo, K. Yang, J.Y. Lin, J.J. Gao, X.Y. Wu, Z.Y. Wang, Synthesis of amino acid derivatives of 5-alkoxy-3,4-dihalo-2(5H)-furanones and their preliminary bioactivity investigation as linkers, *Org. Biomol. Chem.* 17 (2019) 5138–5147, <https://doi.org/10.1039/C9OB00736A>.
- [6] Z.H. Wang, Y. You, Y.Z. Chen, X.Y. Xu, W.C. Yuan, An asymmetric organo-catalytic vinyllogous Mannich reaction of 3-methyl-5-arylfuran-2(3H)-ones with *N*-(2-pyridinesulfonyl) imines: enantioselective synthesis of δ -amino γ,γ -disubstituted butenolides, *Org. Biomol. Chem.* 16 (2018) 1636–1640, <https://doi.org/10.1039/C8OB03117C>.
- [7] Z.Z. Li, H. Su, W.W. Yu, X.J. Li, H. Cheng, M.Y. Liu, X.F. Pang, X.Z. Zou, Design, synthesis and anticancer activities of novel otobain derivatives, *Org. Biomol. Chem.* 14 (2016) 277–287, <https://doi.org/10.1039/C5OB02176F>.
- [8] P. Yang, M. Yao, J. Li, Y. Li, A. Li, Total synthesis of rubrifloridilactone B, *Angew. Chem. Int. Ed.* 55 (2016) 6964–6968, <https://doi.org/10.1002/anie.201601915>.
- [9] Q.A. Castillo, J. Triana, J.L. Eiroa, L. Calcul, E. Rivera, L. Wojtas, J.M. Padron, L. Boberioth, M. Keramane, E. AbelSantos, L.A. Baez, E.A. Germosen, *ent*-Labdane diterpenoids from the aerial parts of *Eupatorium obtusissimum*, *J. Nat. Prod.* 79 (2016) 907–913, <https://doi.org/10.1021/acs.jnatprod.5b00954>.
- [10] J. Luo, H.F. Wang, X. Han, L.W. Xu, J. Kwiatkowski, K.W. Huang, Y.X. Lu, The direct asymmetric vinyllogous Aldol reaction of furanones with α -ketoesters: access to chiral γ -butenolides and glycerol derivatives, *Angew. Chem. Int. Ed.* 50 (2011) 1861–1864, <https://doi.org/10.1002/anie.201006316>.
- [11] M.-X. Wei, J. Zhang, F.-L. Ma, M. Li, J.-Y. Yu, W. Luo, X.-Q. Li, Synthesis and biological activities of dithiocarbamates containing 2(5H)-furanone-piperazine, *Eur. J. Med. Chem.* 155 (2018) 165–170, <https://doi.org/10.1016/j.ejmech.2018.05.056>.
- [12] M.-X. Wei, L. Feng, X.-Q. Li, X.-Z. Zhou, Z.-H. Shao, Synthesis of new chiral 2,5-disubstituted 1,3,4-thiadiazoles possessing γ -butenolide moiety and preliminary evaluation of in vitro anticancer activity, *Eur. J. Med. Chem.* 44 (2009) 3340–3344, <https://doi.org/10.1016/j.ejmech.2009.03.023>.
- [13] U. Eckstein-Ludwig, R.J. Webb, I.D.A. van Goethem, J.M. East, A.G. Lee, M. Kimura, P.M. O'Neill, P.G. Bray, S.A. Ward, S. Krishna, Artemisinins target the SERCA of *Plasmodium falciparum*, *Nature* 424 (2003) 957–961, <https://doi.org/10.1038/nature01813>.
- [14] R.K. Haynes, B. Fugmann, J. Stetter, K. Rieckmann, H.D. Heilmann, H.W. Chan, M.K. Cheung, W.L. Lam, H.N. Wong, S.L. Croft, L. Vivas, L. Rattray, L. Stewart, W. Peters, B.L. Robinson, M.D. Edstein, B. Kotecka, D.E. Kyle, B. Beckermann, M. Gerisch, M. Radtke, G. Schmuck, W. Steinke, U. Wollborn, K. Schmeer, A. Römer, Artemisone—a highly active antimalarial drug of the artemisinin class, *Angew. Chem. Int. Ed.* 45 (2006) 2082–2088, <https://doi.org/10.1002/anie.200503071>.
- [15] Y.K. Wong, C. Xu, K.A. Kalesh, Y. He, Q. Lin, W.S.F. Wong, H.M. Shen, J. Wang, Artemisinin as an anticancer drug: recent advances in target profiling and mechanisms of action, *Med. Res. Rev.* 37 (2017) 1492–1517, <https://doi.org/10.1002/med.21446>.
- [16] Z. Jiang, J. Chai, H.H.F. Chuang, S. Li, T. Wang, Y. Cheng, W. Chen, D. Zhou, Artesunate induces G0/G1 cell cycle arrest and iron-mediated mitochondrial apoptosis in A431 human epidermoid carcinoma cells, *Anti Canc. Drugs* 23 (2012) 606–613, <https://doi.org/10.1097/CAD.0b013e328350e8ac>.
- [17] H. Sun, X. Meng, J. Han, Z. Zhang, B. Wang, X. Bai, X. Zhang, Anti-cancer activity of DHA on gastric cancer—an in vitro and in vivo study, *Tumor. Biol.* 34 (2013) 3791–3800, <https://doi.org/10.1007/s13277-013-0963-0>.
- [18] A. Bhaw-Luximon, D. Jhurry, Artemisinin and its derivatives in cancer therapy: status of progress, mechanism of action, and future perspectives, *Canc. Chemother. Pharmacol.* 79 (2017) 451–466, <https://doi.org/10.1007/s00280-017-3251-7>.
- [19] H.J. Zhou, J.L. Zhang, A. Li, Z. Wang, X.E. Lou, Dihydroartemisinin improves the efficiency of chemotherapeutics in lung carcinomas in vivo and inhibits murine Lewis lung carcinoma cell line growth in vitro, *Canc. Chemother. Pharmacol.* 66 (2010) 21–29, <https://doi.org/10.1007/s00280-009-1129-z>.
- [20] P.C.H. Li, E. Li, W.P. Roos, M.Z. Zdzenicka, B. Kaina, T. Efferth, Artesunate derived from traditional Chinese medicine induces DNA damage and repair, *Canc. Res.* 68 (2008) 4347–4351, <https://doi.org/10.1158/0008-5472.CAN-07-2970>.
- [21] X. Feng, L. Li, H. Jiang, K. Jiang, Y. Jin, J. Zheng, Dihydroartemisinin potentiates the anticancer effect of cisplatin via mTOR inhibition in cisplatin-resistant ovarian cancer cells: involvement of apoptosis and autophagy, *Biochem. Biophys. Res. Co.* 444 (2014) 376–381, <https://doi.org/10.1016/j.bbrc.2014.01.053>.
- [22] J.-Y. Yu, X.-Q. Li, M.-X. Wei, Synthesis and biological activities of artemisinin-piperazine-dithiocarbamate derivatives, *Eur. J. Med. Chem.* 169 (2019) 21–28, <https://doi.org/10.1016/j.ejmech.2019.02.071>.

- [23] T. Efferth, Cancer combination therapies with artemisinin-type drugs, *Biochem. Pharmacol.* 139 (2017) 56–70, <https://doi.org/10.1016/j.bcp.2017.03.019>.
- [24] T. Fröhlich, A. Kiss, J. Wölfling, E. Mernyák, Á.E. Kulmány, R. Minorics, I. Zupkó, M. Leidenberger, O. Friedrich, B. Kappes, F. Hahn, M. Marschall, G. Schneider, S.B. Tsogoeva, Synthesis of artemisinin–estrogen hybrids highly active against HCMV, *P. falciparum*, and cervical and breast cancer, *ACS Med. Chem. Lett.* 9 (2018) 1128–1133, <https://doi.org/10.1021/acsmchemlett.8b00381>.
- [25] E. Ooko, M.E.M. Saeed, O. Kadioglu, S. Sarvi, M. Colak, K. Elmasaoudi, R. Janah, H.J. Greten, T. Efferth, Artemisinin derivatives induce iron-dependent cell death (ferroptosis) in tumor cells, *Phytomedicine* 22 (2015) 1045–1054, <https://doi.org/10.1016/j.phymed.2015.08.002>.
- [26] J. Chen, Z. Guo, H.-B. Wang, J.-J. Zhou, W.-J. Zhang, Q.-W. Chen, Multifunctional mesoporous nanoparticles as pH-responsive Fe²⁺ reservoirs and artemisinin vehicles for synergistic inhibition of tumor growth, *Biomaterials* 35 (2014) 6498–6507, <https://doi.org/10.1016/j.biomaterials.2014.04.028>.
- [27] T. Efferth, A. Benakis, M.R. Romero, M. Tomić, R. Rauh, D. Steinhach, R. Hafer, T. Stamminger, F. Oesch, B. Kaina, M. Marschall, Enhancement of cytotoxicity of artemisinins toward cancer cells by ferrous iron, *Free Radical Bio. Med* 37 (2004) 998–1009, <https://doi.org/10.1016/j.freeradbiomed.2004.06.023>.
- [28] X.-R. Deng, Z.-X. Liu, F. Liu, L. Pan, H.-P. Yu, J.-P. Jiang, J.-J. Zhang, L. Liu, J. Yu, Holotransferrin enhances selective anticancer activity of artemisinin against human hepatocellular carcinoma cells, *J. Huazhong Univ. Sci. Technol. - Med. Sci.* 33 (2013) 862–865, <https://doi.org/10.1007/s11596-013-1212-x>.
- [29] T. Efferth, Artemisinin—second career as anticancer drug, *World, J. Tradit. Chin. Med.* 1 (2015) 2–25, <https://doi.org/10.15806/j.issn.2311-8571.2015.0036>.
- [30] M.-X. Wei, C. Ma, C.-X. Chen, J. Xu, H. Zhang, X.-Q. Li, Syntheses and preliminary anti-cancer activities of novel dihydroartemisinin-piperazine derivatives containing amide, *Huaxue Tongbao* 78 (2015) 1090–1095, <https://doi.org/10.14159/j.cnki.0441-3776.2015.12.003>.
- [31] A. Byczek-Wyrostek, R. Kitel, K. Rumak, M. Skonieczna, A. Kasprzycka, K. Walczak, Simple 2(5*H*)-furanone derivatives with selective cytotoxicity towards non-small cell lung cancer cell line A549 - synthesis, structure-activity relationship and biological evaluation, *Eur. J. Med. Chem.* 150 (2018) 687–697, <https://doi.org/10.1016/j.ejmech.2018.03.021>.
- [32] X.-M. Song, Z.-Y. Wang, J.-X. Li, J.-H. Fu, Tandem reaction of 5-Alkoxy-3,4-dihalo-5*H*-furan-2-one with α,ω -diamines, *Chin. J. Org. Chem.* 29 (2009) 1804–1810, http://sioc-journal.cn/jwk_yjhx/CN/Y2009/V29/I11/1804.
- [33] Q.-H. Chen, Z. Geng, A new chiral source optically pure 5-(1-menthyloxy)-3,4-dichloro-2(5*H*)-furanone, its synthesis and structure, *Hua Hsueh Hsueh Pao* 51 (1993) 622–624, http://sioc-journal.cn/jwk_hxxb/CN/Y1993/V51/I6/662.
- [34] X.-Q. Li, Q.-H. Chen, Synthesis and structure of the chiral dialkyl phosphonate derivatives, *Chem. J. Chin. Univ.* 22 (2001) 1677–1681, <http://www.cjcu.jlu.edu.cn/CN/Y2001/V22/I10/1677>.
- [35] Q.H. Chen, Z. Geng, B. Huang, Synthesis of enantiomerically pure 5-(1-menthyloxy)-3,4-dibromo-2(5*H*)-furanone and its tandem asymmetric Michael addition-elimination reaction, *Tetrahedron: Asymmetry* 6 (1995) 401–404, [https://doi.org/10.1016/0957-4166\(95\)00024-J](https://doi.org/10.1016/0957-4166(95)00024-J).